

# Room temperature hydrolysis of benzamidines and benzamidiniums in weakly basic water

Li-Juan Yu,<sup>a</sup> Duncan A. Cullen,<sup>a</sup> Mahbod Morshedi,<sup>a</sup> Michelle L. Coote,<sup>a\*</sup> and Nicholas G. White<sup>a\*</sup>

<sup>a</sup> Research School of Chemistry, Australian National University, Canberra, ACT, 2600, Australia

\* Email: michelle.coote@anu.edu.au, nicholas.white@anu.edu.au

Benzamidinium compounds have found widespread use in both medicinal and supramolecular chemistry. In this work, we show that benzamidiniums hydrolyse at room temperature in aqueous base to give the corresponding primary amide. This reaction has a half-life of 300 days for unsubstituted benzamidinium at pH 9, but is relatively rapid at higher pHs (e.g.  $t_{1/2}$  = 6 days at pH 11 and 15 hours at pH 13). Quantum chemistry combined with first principles kinetic modelling can reproduce these trends and explain them in terms of the dominant pathway being initiated by attack of HO<sup>-</sup> on benzamidine. Incorporation of the amidinium motif into a hydrogen bonded framework offers a substantial protective effect against hydrolysis.

## Introduction

Compounds based on benzamidine or protonated benzamidinium functional groups are used in a wide range of biological and medicinal chemistry applications, and are seeing increasing use in supramolecular chemistry.<sup>1,2</sup> The high basicity of amidine and benzamidine derivatives means that they are protonated under physiological conditions and as a result have high water solubility, but potentially low bioavailability.

Numerous drug molecules contain some form of amidine/amidinium functionality, and many are based on benzamidinium groups.<sup>3</sup> Indeed, unsubstituted benzamidinium is an effective trypsin inhibitor,<sup>4</sup> and several benzamidinium molecules have been developed as reversible serine protease inhibitors, acting by hydrogen bonding to a carboxylate residue in the enzymes' active site.<sup>3, 5, 6</sup> A wide range of drug molecules containing two benzamidinium moieties attached through simple linker groups are available, perhaps most notably pentamidine (Figure 1),<sup>7, 8</sup> which is a World Health Organization Essential Medicine used for treatment of protozoan infections.

Benzamidinium groups have also proven useful in supramolecular chemistry, both in the context of host-guest chemistry and in self-assembly. Early studies by Nocera,<sup>9</sup> Gale<sup>10, 11</sup> and Diederich<sup>12, 13</sup> demonstrated that strong interactions were possible between the benzamidinium group and carboxylates in solution (including polar organic solvents and water), and these and similar interactions have subsequently been used to prepare a range of self-assembled structures. Notably, Crego-Calama's group pioneered the development of capsules based on benzamidinium...carboxylate and benzamidinium...sulfonate interactions,<sup>14, 15</sup> and Yashima has developed a range of structures including catenanes, helices and capsules assembled *via* benzamidinium...carboxylate hydrogen bonds.<sup>16-19</sup> More recently, our group<sup>20-22</sup> and the groups of Ben and

Comotti<sup>23, 24</sup> have demonstrated that benzamidinium groups can be used to form hydrogen bonded frameworks with carboxylate and sulfonate anions.

Given the relevance of these functional groups in both medicinal and supramolecular chemistry, it is important to understand their stability. Lewis and Wolfenden have completed a detailed study of the decomposition of alkylamidine and alkylguanidine derivatives at elevated temperatures: they showed that decomposition in water occurred *via* hydrolysis rather than elimination. Importantly, protonation of the neutral amidine/guanidine species dramatically slowed decomposition.<sup>25</sup> We also note that commercially-available benzamidinium chloride is noted by at least one manufacturer to be sensitive to oxidation in aqueous solution.<sup>26</sup>

In certain circumstances, we have isolated amide-containing products when starting from benzamidiniums. In this report, we investigate the hydrolysis of benzamidiniums at room temperature. We show that while the rate of hydrolysis is negligible at neutral pH, it becomes significant under mildly basic conditions and rapid in strong aqueous base (e.g.  $t_{1/2}$  = 15 hrs at room temperature at pH 13). We do not observe any evidence for oxidation, even upon standing for extended periods in O<sub>2</sub>-saturated D<sub>2</sub>O.<sup>27</sup>

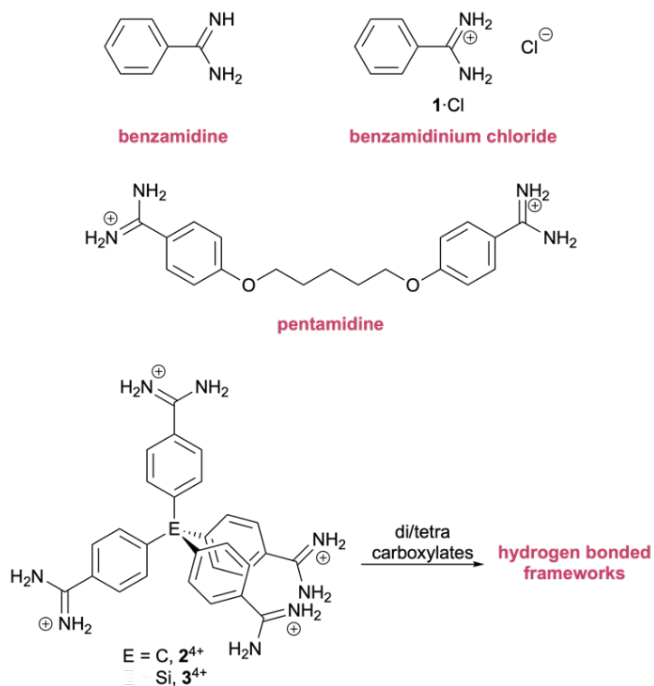


**Figure 1** Structure of benzamidine, benzamidinium, and pentamidine, and diagram showing the use of poly-amidiniums to prepare hydrogen bonded frameworks.

## Results and discussion

**Isolation of tetra-amides from tetra-amidinium crystallisations:** Our group has prepared a range of hydrogen bonded frameworks from benzamidinium and carboxylate tectons. We typically prepare the tetrabutylammonium (TBA) salts of the carboxylates and use these in the reaction, however we were interested to see whether it was possible to directly use the carboxylic acids and deprotonate *in situ* using an aqueous base such as NaOH or NH<sub>3</sub>. In many cases, this is possible, and indeed we have used this methodology when encapsulating enzymes within our hydrogen bonded frameworks.<sup>28</sup> However, when we tried to make frameworks from the tetra-amidinium **2<sup>4+</sup>** and anthracenedicarboxylate or bromoterephthalate in this way,<sup>29</sup> we obtained single crystals not of the desired hydrogen bonded frameworks but of the tetra-amide compound **4** (Figure 2). Similarly, when we attempted to prepare frameworks from the silicon-centred tetra-amidinium **3<sup>4+</sup>** and bicarbonate, we sometimes obtained crystals of the silicon tetra-amide **5**. It was notable that in both of these cases, crystallization took a long time (several days). In fact in the case of the silicon-based system, if we used higher concentrations, crystallization occurred more rapidly and we did not obtain the tetra-amide **5**, but instead obtained a hydrogen bonded salt of the tetra-amidinium.<sup>30</sup>

The crystal structures of **4** and **5** are isostructural and crystallize in the tetragonal space group  $P4_2/n$ . The structures assemble through N–H···O=C amide···amide hydrogen bonds, which have a double helical arrangement (Figure 2). While related systems based on self-complementary hydrogen bonds and tetraphenylmethane or tetraphenylsilane components form

large solvent-filled channels,<sup>31-33</sup> **4** and **5** are close-packed and do not contain any solvent. Attempts to synthesize bulk **4** or **5** by standing **2·Cl<sub>4</sub>** or **3·Cl<sub>4</sub>** in aqueous base did not result in clean conversion; the solid products appeared to be contaminated with amidine derivatives, *i.e.* on a bulk scale precipitation occurs before complete conversion to the amide.

**NMR study of hydrolysis of benzamidinium:** To gain an understanding of the decomposition process, we initially investigated the hydrolysis of benzamidinium chloride (**1·Cl**) using <sup>1</sup>H NMR experiments in D<sub>2</sub>O. We initially studied what happened when **1·Cl** was exposed to the relatively weak bases, sodium hydrogencarbonate and sodium carbonate. After 24 hrs in the presence of one equivalent of Na<sub>2</sub>CO<sub>3</sub>, approximately 15% of the benzamidinium cation had been hydrolysed to give benzamide, rising to approximately 50% after eight days. When only 10 mol% Na<sub>2</sub>CO<sub>3</sub> was present, hydrolysis was slower with only 6% hydrolysis within 24 hours and 20% hydrolysis after eight days. In contrast hydrolysis was very slow when NaHCO<sub>3</sub> was used (approximately 10% hydrolyzed after three weeks in the presence of four equivalents of NaHCO<sub>3</sub>).

Given the apparent dependence on pH, we next studied hydrolysis of **1·Cl** in deuterated buffers. At pH 10, negligible hydrolysis was observed in the first few hours and after 30 hours, less than 2% of **1<sup>+</sup>** had been hydrolyzed. Increasing pH dramatically increased the rate of hydrolysis, with 11% of **1<sup>+</sup>** hydrolyzed after 30 hours at pH 11, and 36% of **1<sup>+</sup>** hydrolyzed after 30 hours at pH 12 (Figure 3). Rate constants for these reactions are provided in Table 1, as well as rate constants in aqueous hydroxide (0.10 or 1.0 M), which are faster again. Interestingly the rate does not increase substantially on going from 0.10 to 1.0 M NaOH<sub>(aq)</sub>, and these rates are only slightly faster than phosphate buffer at pH = 12.

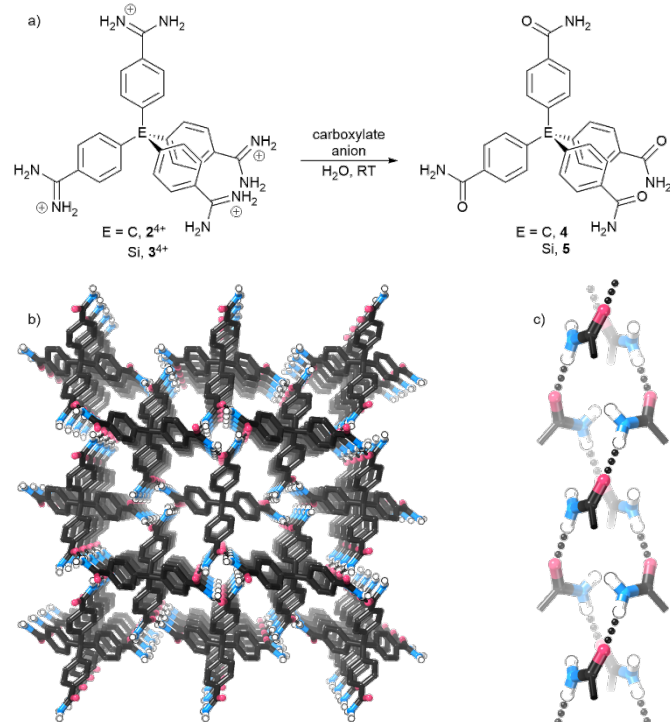


**Figure 2** a) Conversion of tetra-amidiniums to single crystals of tetra-amides; b) diagram showing packing in crystal structure of **4** (C–H hydrogen atoms omitted for clarity), c) diagram showing double helical hydrogen bonding arrangement in crystal structure of **4**. The structure of **5** is isostructural with **4** (Figures S3 and S4).

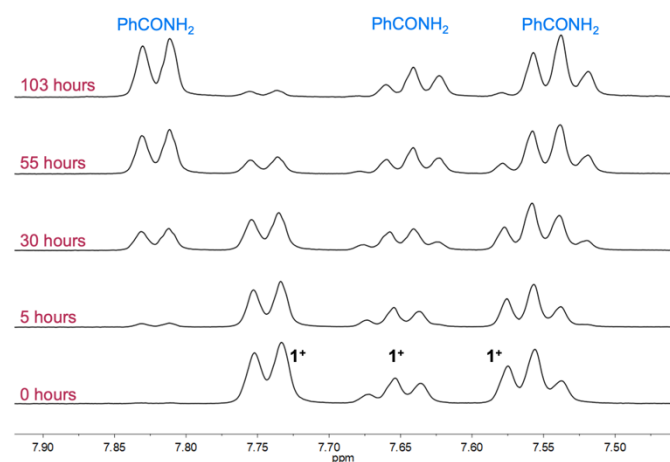


**Figure 3** Truncated  $^1\text{H}$  NMR spectra showing conversion of  $1^+$  to benzamide (10 mM  $1\text{-Cl}$  in 100 mM phosphate buffer at pH = 12 in  $\text{D}_2\text{O}$ , 400 MHz, 298 K).

**Table 1** Rate constants for hydrolysis of  $1\text{-Cl}$ .

Condition	Rate constant, $k$ ( $\text{s}^{-1}$ ) <sup>a</sup>	$t_{1/2}$
Buffer, <sup>b</sup> pH = 9	$2.7(6) \times 10^{-8}$	300 days
Buffer, <sup>b</sup> pH = 10	$1.7(2) \times 10^{-7}$	47 days
Buffer, <sup>b</sup> pH = 11	$1.3(1) \times 10^{-6}$	6 days
Buffer, <sup>b</sup> pH = 12	$6.0(2) \times 10^{-6}$	32 hrs
0.10 M NaOH <sup>c</sup> initial pH = 13	$1.3(1) \times 10^{-5}$	15 hrs
1.0 M NaOH <sup>c</sup> initial pH = 14	$1.4(1) \times 10^{-5}$	14 hrs

<sup>a</sup> Estimated standard errors of the regression are given in parentheses. <sup>b</sup> 10 mM  $1\text{-Cl}$ , 100 mM phosphate buffer in  $\text{D}_2\text{O}$ . <sup>c</sup> 10 mM  $1\text{-Cl}$  and NaOH in  $\text{D}_2\text{O}$ .

**Computational Study.** To understand the pH-dependence of the hydrolysis rate, density functional theory calculations were performed at the M062X/Def2-TZVP//M06-2X/6-31+G(d,p) level of theory using an SMD-based cluster continuum model to take into account solvent effects in water. A previous theoretical study of this substrate only considered reactions with water,<sup>34</sup> though experimental<sup>25</sup> and computational<sup>35</sup> studies of related substrates suggest  $\text{HO}^-$  attack is likely to be involved, at least at some pH values.

Thus, in the present work five pathways were considered corresponding to initial attack by either  $\text{HO}^-$  or  $\text{H}_2\text{O}$  on either benzamidinium or benzamidine. In the latter case, two different pathways for  $\text{HO}^-$  attack were considered, one of which involves a subsequent  $\text{H}^+$  attack during the hydrolysis and is labelled  $\text{HO}^- / \text{H}^+$ . For each pathway, pseudo first order rate coefficients were calculated as a function of pH using analytical steady state kinetic models, that were derived based on the reasonable assumption that the final step in the process was irreversible, and that the concentrations of  $[\text{HO}^-]$  and  $[\text{H}^+]$  remained constant. Full methodological details and results are provided in the Supporting Information. Table 2 provides the rate coefficients for each pathway as a function of pH, as well as the overall weighted rate coefficient, weighted by the speciation of benzamidinium versus benzamidine at each pH, as calculated using the experimental  $\text{pK}_a$  of benzamidinium (11.6).<sup>36</sup>

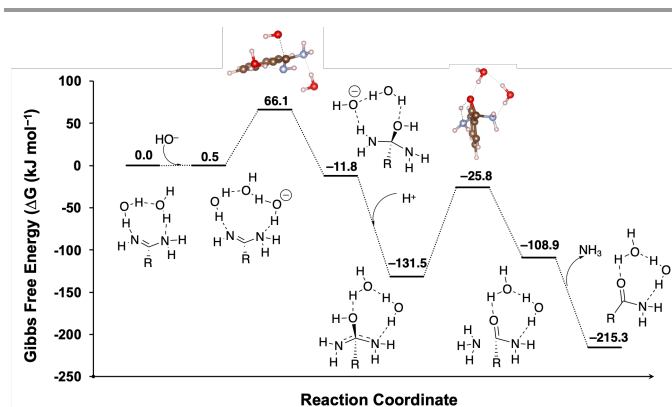


Figure 4. The potential energy surface ( $\Delta G$ ,  $\text{kJ mol}^{-1}$ , 298 K,  $\text{H}_2\text{O}$ ) of  $\text{HO}^-$  attacking benzamidine followed by protonation of intermediate. The two transition states are shown as ball and stick figures.

The dominant pathway involves  $\text{HO}^-$  attack on the benzamidine, followed by protonation of the intermediate. This pathway is shown in Figure 4, while all individual steps of all pathways are shown in Scheme S1. Even at low pH where the benzamidine concentration is 400 times smaller than the benzamidinium, the hydrolysis of benzamidine still makes the major contribution to the weighted rate coefficient. Consistent with this picture, sensitivity analysis (Table S2, Supporting Information) revealed that increasing or decreasing the various individual rate coefficients in the benzamidinium  $\text{HO}^-$  pathway by an order of magnitude had a negligible impact ( $< 5\%$ ) on the overall half-life. This was also true of the benzamidine  $\text{HO}^-$  pathway, except at very high pH, where order of magnitude changes to all three rate coefficients ( $k_1$ ,  $k_{-1}$ ,  $k_2$ ) resulted in changes to the half-life of 40-80%. However, equivalent changes to these same three rate coefficients ( $k_1$ ,  $k_{-1}$ ,  $k_2$ ) in the benzamidine  $\text{HO}^-/\text{H}^+$  pathway affected the half-life

by up to 900% across the entire pH range. These first steps are rate controlling, with order of magnitude changes to the rate coefficients for the later steps in this pathway ( $k_{-2}$  and  $k_3$ ) having a negligible effect on the overall half-life.

The low pH sensitivity of this dominant pathway stems from the fact that the first step involves attack by  $\text{HO}^-$  but the subsequent step involves protonation. As both of these steps are rate controlling, the resulting rate coefficient for benzamidine is largely pH independent. The pH dependence of overall hydrolysis rate is thus governed largely by the pH dependence of the benzamidinium:benzamidine speciation. As a result, we predict computationally a smooth decrease in half-life as pH increases, and these results agree well with experiment (Figure 5).

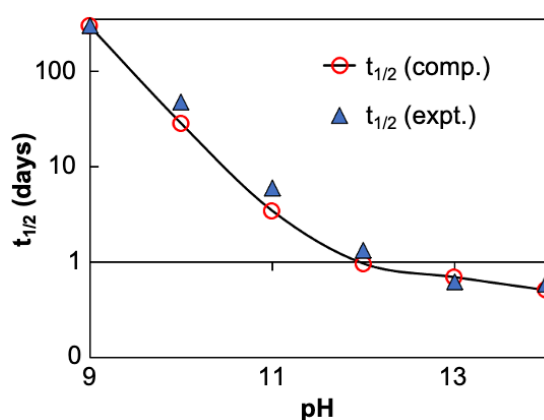


Figure 5 Comparison of computational and experimental half-lives for hydrolysis of 1-Cl.

Table 2 Computed pseudo-first order rate constants for hydrolysis of 1<sup>a</sup>.

pH	$\frac{[\text{benzamidine}]}{[\text{benzamidinium}]}$	Rate constant, $k$ ( $\text{s}^{-1}$ )						overall	half-life
		benzamidinium		benzamidine					
		$\text{H}_2\text{O}$	$\text{HO}^-$	$\text{H}_2\text{O}$	$\text{HO}^-$	$\text{HO}^-/\text{H}^+$			
9	$2.51 \times 10^{-3}$	$8.22 \times 10^{-12}$	$5.27 \times 10^{-12}$	$1.91 \times 10^{-20}$	$4.29 \times 10^{-11}$	$1.09 \times 10^{-5}$	$2.73 \times 10^{-8}$	294 days	
10	$2.51 \times 10^{-2}$	$2.61 \times 10^{-11}$	$5.27 \times 10^{-11}$	$1.91 \times 10^{-20}$	$4.29 \times 10^{-10}$	$1.16 \times 10^{-5}$	$2.84 \times 10^{-7}$	28 days	
11	$2.51 \times 10^{-1}$	$3.34 \times 10^{-11}$	$5.27 \times 10^{-10}$	$1.91 \times 10^{-20}$	$4.29 \times 10^{-9}$	$1.17 \times 10^{-5}$	$2.34 \times 10^{-6}$	82 hrs	
12	2.51	$3.43 \times 10^{-11}$	$5.27 \times 10^{-9}$	$1.91 \times 10^{-20}$	$4.29 \times 10^{-8}$	$1.17 \times 10^{-5}$	$8.38 \times 10^{-6}$	23 hrs	
13	25.1	$3.44 \times 10^{-11}$	$5.27 \times 10^{-8}$	$1.91 \times 10^{-20}$	$4.29 \times 10^{-7}$	$1.17 \times 10^{-5}$	$1.16 \times 10^{-5}$	17 hrs	
14	251	$3.44 \times 10^{-11}$	$5.27 \times 10^{-7}$	$1.91 \times 10^{-20}$	$4.29 \times 10^{-6}$	$1.17 \times 10^{-5}$	$1.59 \times 10^{-5}$	12 hrs	

<sup>a</sup> Calculated using quantum-chemical predicted rate and equilibrium coefficients for the individual steps in each hydrolysis pathway shown in Scheme S1 of the Supporting Information. The solution was assumed to be buffered at the specified pH for all calculations. The overall rate coefficient for hydrolysis is calculated as a weighted sum of those for benzamidinium and benzamidine, weighted by their speciation at the given pH.

**NMR study of hydrolysis of poly-amidiniums:** We were interested to see how charge affects the rate of hydrolysis of polycationic species such as  $2^{4+}$  and the bis-amidinium  $6^{2+}$ . Unfortunately, it was not possible to study  $2^{4+}$  or  $6^{2+}$  in phosphate buffer, as they did not dissolve, which we attribute to the formation of insoluble (hydrogen)phosphate-containing networks. The same thing was observed when we attempted to use carbonate as base to study the hydrolysis of  $2^{4+}$ , which we attribute to a similar phenomenon. The compounds  $2^{4+}$  and  $6^{2+}$  also did not dissolve in aqueous sodium hydroxide, which we attribute to formation of the insoluble bis/tetra-amidines.<sup>37</sup>

Using 1%  $\text{NH}_3$  in  $\text{D}_2\text{O}$ , we were able to study the hydrolysis of  $1^+$ ,  $2^{4+}$  and  $6^{2+}$ . When  $1^+$  was studied, all species stay in solution; however hydrolysis of  $2^{4+}$  and  $6^{2+}$  gives insoluble products, so we studied the disappearance of the starting material against a 1,4-dioxane standard. The rate of hydrolysis of  $1^+$  in this solvent was  $1.7(1) \times 10^{-6} \text{ s}^{-1}$ , *i.e.* between the rates of buffer at pH 11 and 12, as would be expected given the pH of 1%  $\text{NH}_3$  in  $\text{D}_2\text{O}$  (~11.5). Both the bis-amidinium  $6^{2+}$  and tetra-amidinium  $2^{4+}$  hydrolyzed more rapidly than  $1^+$ , by a factor of approximately four for  $6^{2+}$  and three for  $2^{4+}$  (Table 3). These systems are not directly comparable with one another, as both amidinium moieties are attached to the same benzene ring in  $6^{2+}$ , while in  $2^{4+}$  the four amidinium moieties are on separate rings. Nevertheless, it is clear that poly-amidinium compounds hydrolyze more rapidly than simple  $1^+$ .

**Table 3** Rate constants for hydrolysis amidinium species in 1%  $\text{NH}_3(\text{aq})$ .<sup>a</sup>

Compound	Rate constant, $k$ ( $\text{s}^{-1}$ ) <sup>a</sup>	$t_{1/2}$
1-Cl	$1.7(1) \times 10^{-6}$	5 days
2-Cl <sub>4</sub>	$5.4(2) \times 10^{-6}$	36 hrs
6-Cl <sub>2</sub>	$6.6(3) \times 10^{-6}$	29 hrs

<sup>a</sup> All compounds 10 mM, 1%  $\text{NH}_3$  is approximately 540 mM and has a pH of approximately 11.5. <sup>b</sup> Estimated standard errors of the regression are given in parentheses.

**NMR study of hydrolysis of amidinium carboxylate frameworks:** We were interested to see how robust amidinium...carboxylate frameworks are in the presence of base. We have previously demonstrated that enzymes encapsulated in frameworks are stable at pH 4–10, but decompose at pH 14.<sup>28</sup> We also only observed formation of **4** from  $2^{4+}$  when crystals of the amidinium...carboxylate framework did not form rapidly – both of which suggest that crystallization may offer some form of protection against hydrolysis. To study this, we studied two hydrogen bonded frameworks: a 2D material formed from  $6^{2+}$  and terephthalate,<sup>38, 39</sup> and a 3D network formed from  $2^{4+}$  and tetrakis(4-carboxyphenyl)methane<sup>20</sup> (see Supporting Information for structures).

Suspensions of these frameworks (10 mM) in 1%  $\text{NH}_3$  in  $\text{D}_2\text{O}$  were stored at room temperature for seven days, and monitored by  $^1\text{H}$  NMR spectroscopy. If the amidinium compound decomposed, it would be expected that this would

release the carboxylate into aqueous solution, however negligible leaching of any organic compounds into solution was observed. After seven days, the suspensions were filtered and the solid material analyzed by powder X-ray diffraction (PXRD), which revealed that both frameworks remained crystalline during this treatment (Figures S42 and S43). The solid materials were digested with  $\text{DCl}(\text{aq})$ , dissolved in  $d_6$ -DMSO and analyzed by  $^1\text{H}$  NMR spectroscopy. This revealed negligible decomposition for the framework assembled from  $6^{2+}$ , and minimal (~5%) decomposition for the framework prepared from  $2^{4+}$ . It appears that incorporation into a solid state framework offers a significant protective effect, given that free  $6^{2+}$  and  $2^{4+}$  are > 95% hydrolyzed within one week. When the frameworks were suspended in 100 mM  $\text{NaOH}(\text{aq})$  (*i.e.* a starting pH of 13), significant decomposition was observed.

## Conclusions

Benzamidinium containing molecules hydrolyze relatively rapidly at room temperature in weakly basic water, but do not appear to oxidize under these conditions. The rate of hydrolysis increases with increasing pH, primarily due to the effect of pH on the protonation state of the benzamidinium. DFT calculations combined with kinetic modelling reproduces the experimental results and indicates that the dominant pathway over the pH range studied (pH 9 – 14) is  $\text{HO}^-$  attack on the benzamide, followed by protonation of the intermediate species prior to hydrolysis. This individual pathway has a rate coefficient that is largely pH independent, but its rate declines with decreasing pH as benzamide is increasingly protonated into its less reactive benzamidinium form. As a result, incorporating benzamidinium groups into a hydrogen bonded framework offers significant protection against hydrolysis.

## Experimental Section

Benzamidinium chloride hydrate was recrystallized from 1.0 M  $\text{HCl}(\text{aq})$  before use.<sup>40</sup> Characterization by X-ray crystallography revealed that crystals fresh from the mother liquor were the dihydrate, while thermogravimetric analysis indicated that the dried product was the monohydrate (see Supporting Information). The tetra-amidinium compounds  $2^{4+}$ ,<sup>22</sup> and  $3^{4+}$ ,<sup>30</sup> and the bis-amidinium  $6^{2+}$ ,<sup>38</sup> were prepared as previously described, as were the hydrogen bonded frameworks assembled from  $6^{2+}$  and terephthalate,<sup>39</sup> and from  $2^{4+}$  and tetrakis(4-carboxyphenyl)methane.<sup>20</sup> Other compounds were bought from commercial suppliers and used as received.

## Computational methods

All the geometry optimizations and single point energy calculations were performed with the Gaussian 16 software package.<sup>41</sup> Geometries were optimized in water at the M06-

2X/6-31+G(d,p) level of theory<sup>42</sup> with SMD solvent model,<sup>43</sup> and frequencies were also calculated at this level. Geometries were verified either as local minima (possessing no imaginary frequencies) or transition states (possessing only one imaginary frequency). Entropies, thermal corrections, and zero-point vibrational energies were calculated using frequencies scaled by the recommended scaling factors based on solution phase optimized geometries.<sup>44</sup> Improved single-point energies in gas phase were calculated using the Def2-TZVP basis set<sup>45</sup> with the same DFT functional. Reported Gibbs free energies in solution at 298 K were obtained via a thermocycle method in which electronic energy in gas phase at M062X/Def2-TZVP, was combined with entropies, thermal corrections, and zero-point vibrational energies at M062X/6-31+G(d,p), solvation energies calculated at M062X/6-31+G(d,p) with SMD solvent model and the necessary phase change correction term.<sup>46</sup> The rate coefficients for each step are obtained using the Eyring equation in conjunction with the quantum-chemically calculated Gibbs free energy barriers. While tunnelling is likely to play a role in number of the proton-hopping reactions studied here, simple Eckart calculations indicate it is negligible for the rate controlling steps of the benzamidine HO<sup>-</sup>/H<sup>+</sup> pathway and thus it was neglected from the calculations.

## Supporting Information

Supporting Information. Additional characterization data, copies of NMR spectra, details of hydrolysis experiments, details of computational experiments.

## Acknowledgements

We thank the Australian Research Council for financial support (DE170100200 and FL170100041), the National Computational Infrastructure for supercomputing time, and Drs Lara Malins and Tristan Reekie (Australian National University) for helpful discussions.

## References

1. Yashima, E.; Maeda, K.; Furusho, Y., Single- and Double-Stranded Helical Polymers: Synthesis, Structures, and Functions. *Acc. Chem. Res.* **2008**, *41*, 1166-1180.
2. White, N. G., Recent advances in self-assembled amidinium and guanidinium frameworks. *Dalton Trans.* **2019**, *48*, 7062-7068.
3. Greenhill, J. V.; Lue, P., 5. Amidines and Guanidines in Medicinal Chemistry, in *Prog. Med. Chem.*, Ellis, G. P.; Luscombe, D. K., Eds. Elsevier: 1993; Vol. 30, pp 203-326.
4. Mares-Guia, M.; Shaw, E., Studies on the Active Center of Trypsin: The Binding of Amidines and Guanidines as Models of the Substrate Side Chain, *J. Biol. Chem.* **1965**, *240*, 1579-1585.
5. Giovanni, A.; David, P. F., Protease Inhibitors in the Clinic. *Med. Chem.* **2005**, *1*, 71-104.
6. Schiebel, J.; Gaspari, R.; Wulsdorf, T.; Ngo, K.; Sohn, C.; Schrader, T. E.; Cavalli, A.; Ostermann, A.; Heine, A.; Klebe, G., Intriguing role of water in protein-ligand binding studied by neutron crystallography on trypsin complexes. *Nature Commun.* **2018**, *9*, 3559.
7. Bray, P. G.; Barrett, M. P.; Ward, S. A.; de Koning, H. P., Pentamidine uptake and resistance in pathogenic protozoa: past, present and future. *Trends Parasitol.* **2003**, *19*, 232-239.
8. Soeiro, M. N. C.; Werbovets, K.; Boykin, D. W.; Wilson, W. D.; Wang, M. Z.; Hemphill, A., Novel amidines and analogues as promising agents against intracellular parasites: a systematic review. *Parasitology* **2013**, *140*, 929-951.
9. Deng, Y.; Roberts, J. A.; Peng, S.-M.; Chang, C. K.; Nocera, D. G., The Amidinium–Carboxylate Salt Bridge as a Proton-Coupled Interface to Electron Transfer Pathways. *Angew. Chem. Int. Ed.* **1997**, *36*, 2124-2127.
10. Gale, P. A., Bis-amidinium calixarenes: Templates for self-assembled receptors. *Tetrahedron Lett.* **1998**, *39*, 3873-3876.
11. Camiolo, S.; Gale, P. A.; Ogden, M. I.; Skelton, B. W.; White, A. H., Solid-state and solution studies of bis-carboxylate binding by bis-amidinium calix[4]arenes. *J. Chem. Soc., Perkin Trans. 2* **2001**, 1294-1298.
12. Sebo, L.; Schweizer, B.; Diederich, F., Cleft-Type Diamidinium Receptors for Dicarboxylate Binding in Protic Solvents. *Helv. Chim. Acta* **2000**, *83*, 80-92.
13. Sebo, L.; Diederich, F.; Gramlich, V., Tetrakis(phenylamidinium)-Substituted Resorcin[4]arene Receptors for the Complexation of Dicarboxylates and Phosphates in Protic Solvents. *Helv. Chim. Acta* **2000**, *83*, 93-113.
14. Corbellini, F.; Fiammengo, R.; Timmerman, P.; Crego-Calama, M.; Versluis, K.; Heck, A. J. R.; Luyten, I.; Reinhoudt, D. N., Guest Encapsulation and Self-Assembly of Molecular Capsules in Polar Solvents via Multiple Ionic Interactions. *J. Am. Chem. Soc.* **2002**, *124*, 6569-6575.
15. Corbellini, F.; Di Costanzo, L.; Crego-Calama, M.; Geremia, S.; Reinhoudt, D. N., Guest Encapsulation in a Water-Soluble Molecular Capsule Based on Ionic Interactions. *J. Am. Chem. Soc.* **2003**, *125*, 9946-9947.
16. Tanaka, Y.; Katagiri, H.; Furusho, Y.; Yashima, E., A Modular Strategy to Artificial Double Helices. *Angew. Chem., Int. Ed.* **2005**, *44*, 3867-3870.
17. Ikeda, M.; Tanaka, Y.; Hasegawa, T.; Furusho, Y.; Yashima, E., Construction of Double-Stranded Metallosupramolecular Polymers with a Controlled Helicity by Combination of Salt Bridges and Metal Coordination. *J. Am. Chem. Soc.* **2006**, *128*, 6806-6807.
18. Katagiri, H.; Tanaka, Y.; Furusho, Y.; Yashima, E., Multicomponent Cylindrical Assemblies Driven by Amidinium–Carboxylate Salt-Bridge Formation. *Angew. Chem., Int. Ed.* **2007**, *46*, 2435-2439.
19. Nakatani, Y.; Furusho, Y.; Yashima, E., Amidinium Carboxylate Salt Bridges as a Recognition Motif for Mechanically Interlocked Molecules: Synthesis of an Optically Active [2]Catenane and Control of Its Structure. *Angew. Chem., Int. Ed.* **2010**, *49*, 5463-5467.
20. Boer, S. A.; Morshedi, M.; Tarzia, A.; Doonan, C. J.; White, N. G., Molecular tectonics: a node-and-linker building block approach to a family of hydrogen bonded frameworks. *Chem. Eur. J.* **2019**, *25*, 10006-10012.
21. Morshedi, M.; Ward, J. S.; Kruger, P. E.; White, N. G., Supramolecular frameworks based on 5,10,15,20-tetra(4-carboxyphenyl)porphyrins. *Dalton Trans.* **2018**, *47*, 783-790.

22. Morshedi, M.; Thomas, M.; Tarzia, A.; Doonan, C. J.; White, N. G., Supramolecular anion recognition in water: synthesis of hydrogen-bonded supramolecular frameworks. *Chem. Sci.* **2017**, *8*, 3019-3025.
23. Xing, G.; Bassanetti, I.; Ben, T.; Bracco, S.; Sozzani, P.; Marchiò, L.; Comotti, A., Multifunctional Organosulfonate Anions Self-Assembled with Organic Cations by Charge-Assisted Hydrogen Bonds and the Cooperation of Water. *Cryst. Growth Des.* **2018**, *18*, 2082-2092.
24. Xing, G.; Bassanetti, I.; Bracco, S.; Negroni, M.; Bezuidenhout, C.; Ben, T.; Sozzani, P.; Comotti, A., A double helix of opposite charges to form channels with unique CO<sub>2</sub> selectivity and dynamics. *Chem. Sci.* **2019**, *10*, 730-736.
25. Lewis, C. A.; Wolfenden, R., The Nonenzymatic Decomposition of Guanidines and Amidines. *J. Am. Chem. Soc.* **2014**, *136* (1), 130-136.
26. For example, the Merck website has the following information about benzamidine chloride hydrate: "Benzamidine HCl is sensitive to oxidation. It is recommended to prepare solutions fresh each time in degassed water prior to use. However, frozen aliquots stored under inert gas, to exclude air, may be stable for a short time. Insufficient information is available to assess the shelf-life of a frozen solution."
27. Oxidation of benzamidine/benzamidinium would presumably give the amidoxime; these compounds are often used as pro-drugs for amidines due to the ready reduction of the amidoxime to amidine *in vivo*. Given this, ready oxidation of the amidine would seem unlikely. Clement, B.; Reduction of N-hydroxylated compounds: amidoximes (N-hydroxyamidines) as pro-drugs of amidines, *Drug Metab. Rev.* **2002**, *34*, 565-579.
28. Liang, W.; Carraro, F.; Solomon, M. B.; Bell, S. G.; Amenitsch, H.; Sumby, C. J.; White, N. G.; Falcaro, P.; Doonan, C. J., Enzyme Encapsulation in a Porous Hydrogen-Bonded Organic Framework. *J. Am. Chem. Soc.* **2019**, *141*, 14298-14305.
29. We have been able to prepare hydrogen bonded frameworks from anthracenedicarboxylate and tetra-amidinium **2**<sup>4+</sup> using the TBA salts of the dicarboxylates, see Ref. 20.
30. Boer, S. A.; Yu, L.-J.; Genet, T. L.; Low, K.; Cullen, D. A.; Gardiner, M. G.; Coote, M. L.; White, N. G., What's in an Atom? A Comparison of Carbon and Silicon-Centred Amidinium---Carboxylate Frameworks. *Chem. Eur. J.* **2021**, *27*, 1768-1776.
31. Simard, M.; Su, D.; Wuest, J. D., Use of hydrogen bonds to control molecular aggregation. Self-assembly of three-dimensional networks with large chambers. *J. Am. Chem. Soc.* **1991**, *113*, 4696-4698.
32. Fournier, J.-H.; Maris, T.; Wuest, J. D.; Guo, W.; Galoppini, E., Molecular Tectonics. Use of the Hydrogen Bonding of Boronic Acids to Direct Supramolecular Construction. *J. Am. Chem. Soc.* **2003**, *125*, 1002-1006.
33. Bassanetti, I.; Bracco, S.; Comotti, A.; Negroni, M.; Bezuidenhout, C.; Canossa, S.; Mazzeo, P. P.; Marchiò, L.; Sozzani, P., Flexible porous molecular materials responsive to CO<sub>2</sub>, CH<sub>4</sub> and Xe stimuli. *J. Mater. Chem. A* **2018**, *6*, 14231-14239.
34. Uddin, K. M.; Alrawashdeh, A. I.; Henry, D. J.; Warburton, P. L.; Poirier, R. A., Hydrolytic deamination reactions of amidine and nucleobase derivatives. *Int. J. Quant. Chem.* **2020**, *120*, e26059.
35. Flinn, C.; Poirier, R. A.; Sokalski, W. A., Ab Initio Study of the Deamination of Formamidine. *J. Phys. Chem. A* **2003**, *107*, 11174-11181.
36. Albert, A.; Goldacre, R.; Phillips, J., 455. The strength of heterocyclic bases. *J. Chem. Soc.* **1948**, 2240-2249.
37. Cullen, D. A.; Gardiner, M. G.; White, N. G., A three dimensional hydrogen bonded organic framework assembled through antielectrostatic hydrogen bonds. *Chem. Commun.* **2019**, *55*, 12020-12023.
38. Thomas, M.; Anglim Lagones, T.; Judd, M.; Morshedi, M.; O'Mara, M. L.; White, N. G., Hydrogen bond-Driven Self-Assembly between Amidinium Cations and Carboxylate Anions: A Combined Molecular Dynamics, NMR Spectroscopy, and Single Crystal X-ray Diffraction Study. *Chem. Asian J.* **2017**, *12*, 1587-1597.
39. Nicks, J.; Boer, S. A.; White, N. G.; Foster, J. A., Monolayer nanosheets formed by liquid exfoliation of charge-assisted hydrogen-bonded frameworks. *Chem. Sci.* **2021**, *12*, 3322-3327.
40. Armarego, W. L. F., Chapter 3 - Purification of Organic Chemicals. In *Purification of Laboratory Chemicals (8<sup>th</sup> Ed.)*, Armarego, W. L. F., Ed. Butterworth-Heinemann: 2017; pp 95-634.
41. Frisch, M.; Trucks, G.; Schlegel, H.; Scuseria, G.; Robb, M.; Cheeseman, J.; Scalmani, G.; Barone, V.; Petersson, G.; Nakatsuji, H.; et al. Gaussian 16. Gaussian, Inc. Wallingford, CT: 2016.
42. Zhao, Y.; Truhlar, D. G., The M06 suite of density functionals for main group thermochemistry, thermochemical kinetics, noncovalent interactions, excited states, and transition elements: two new functionals and systematic testing of four M06-class functionals and 12 other functionals. *Theor. Chem. Acc.* **2008**, *120*, 215-241.
43. Marenich, A. V.; Cramer, C. J.; Truhlar, D. G., Universal solvation model based on solute electron density and on a continuum model of the solvent defined by the bulk dielectric constant and atomic surface tensions. *J. Phys. Chem. B* **2009**, *113*, 6378-6396.
44. Alecu, I.; Zheng, J.; Zhao, Y.; Truhlar, D. G., Computational thermochemistry: scale factor databases and scale factors for vibrational frequencies obtained from electronic model chemistries. *J. Chem. Theory Comput.* **2010**, *6*, 2872-2887.
45. Weigend, F.; Ahlrichs, R., Balanced basis sets of split valence, triple zeta valence and quadruple zeta valence quality for H to Rn: Design and assessment of accuracy. *Phys. Chem. Chem. Phys.* **2005**, *7*, 3297-3305.
46. Ho, J.; Klamt, A.; Coote, M. L., Comment on the correct use of continuum solvent models. *J. Phys. Chem. A* **2010**, *114*, 13442-13444.

## Table of Contents Entry:

